SYSTEM IDENTIFICATION OF WRIST STIFFNESS IN PARKINSON'S DISEASE PATIENTS

by

Chris Sprague

B.S. in Electrical Engineering, University of Pittsburgh, 2006

Submitted to the Graduate Faculty of

the School of Engineering in partial fulfillment

of the requirements for the degree of

M.S. in Electrical Engineering

University of Pittsburgh

2007

UNIVERSITY OF PITTSBURGH

SCHOOL OF ENGINEERING

This thesis was presented

by

Chris Sprague

It was defended on

November 19, 2007

and approved by

Zhi-Hong Mao, PhD, Assistant Professor, Department of Electrical and Computer Engineering

J. Robert Boston, PhD, Professor, Department of Electrical and Computer Engineering

Heung-no Lee, PhD, Assistant Professor, Department of Electrical and Computer Engineering

Thesis Advisor: Zhi-Hong Mao, PhD, Assistant Professor, Department of Electrical and Computer Engineering

SYSTEM IDENTIFICATION OF WRIST STIFFNESS IN PARKINSON'S DISEASE PATIENTS

Chris Sprague, M.S.

University of Pittsburgh, 2007

The purpose of this work is to investigate the characteristics of motor control systems in Parkinson's disease patients. ARMAX system identification was performed to identify the intrinsic and reflexive components of wrist stiffness, enabling a better understanding of the problems associated with Parkinson's disease. The results show that the intrinsic stiffness dynamics represent the vast majority of the total stiffness in the wrist joint and that the reflexive stiffness dynamics are attributable to a tremor commonly found in Parkinsons disease patients. It was found that Parkinsonian rigidity, a symptom of Parkinsons disease, interferes with the known and traditional methods for separating intrinsic and reflexive components. Resolving this problem could lead to early detection of Parkinson's disease in patients not exhibiting typical symptoms, analytical measurement of the severity of the disease, and as a testing mechanism for the effectiveness of new medicines.

TABLE OF CONTENTS

1.0 INTRODUCTION 1

2.0 ANALYSIS METHODS 3

2.1 Test Description 3

2.1.1 Apparatus 3

2.1.2 Test Subjects 5

2.1.3 Testing Procedure 5

2.2 Parallel Wrist Stiffness Dynamics 6

2.2.1 Intrinsic Stiffness 6

2.2.2 Reflexive Stiffness 7

2.2.3 Reflexive Component Delay 8

2.3 Parameter Estimation 8

2.3.1 Discretization 8

2.3.2 ARMAX(Autoregressive Moving Average with eXongenous inputs) . . 9

3.0 IDENTIFICATION METHODS 12

3.1 Intrinsic Stiffness Dynamics 12

3.2 Reflexive Delay 14

3.3 Reflexive Stiffness Dynamics 16

3.4 Identification Procedure 17

4.0 RESULTS 19

4.1 Data Preparation 19

4.2 Reflexive Delay 19

4.3 Intrinsic Stiffness 21

4.4 Reflexive Stiffness 27
4.5 Net Torque 30
5.0 DISCUSSION AND CONCLUSION 32
BIBLIOGRAPHY 35

LIST OF TABLES

1 Relxive Delays 20

2 Intrinsic Stiffness Parameters 27

3 Reflexive Stiffness Parameters: Flexion 27

4 Reflexive Stiffness Parameters: Extension 28

5 Net Torque 30

LIST OF FIGURES

1 Test Apparatus 4
2 Pseudo Random Binary Sequence 4
3 Joint Stiffness Parallel Pathway 6
4 Average Signals 14
5 EMG 15
6 Collected Signals 20
7 Reflexive Delay 21
8 Position vs. Intrinsic Torque 22
9 Discrete Derivative Approximation 24
10 Intrinsic Torque 26
11 Reflexive Torque 28
12 Position vs. Reflexive Torque 29
13 Net Torque Comparison 31

1.0 INTRODUCTION

When an active muscle is stretched, the force required to stretch or contract the muscle is proportional to its length. The proportional dependence of muscle force on length exhibits a spring-like property that has been shown to play a key role in the control of movement. To generate external movements about a joint, the net amount of the rotary force, or torque, required is determined by a combination of the contributions of the muscles. In this case, torque is calculated as the product of force times the length of the moment arm for each muscle. The corresponding measure of rotational position of the joint due to the torque is the change in joint angle. Ultimately, the relationship between joint angle and joint torque serves to characterize the musculature of the joint as a whole. This characterization of musculature can be thought of as joint stiffness, or how a joint resists a movement.

Scientific research has been performed in investigating the joint stiffness of various joints of the human body including the shoulder [1], elbow [2] [3], and ankle [4]. The total stiffness of a joint can be separated into intrinsic and reflexive contributions. The intrinsic stiffness will give us insight to the mechanical properties of joints and musculo-skeleton structure. This includes muscle compliance, skin elasticity, and bone/tissue frictional losses. These properties are not dependent on the bodys attempts to control motion. The reflexive stiffness, on the other hand, gives us insight into how the neural system performs the motor control of the muscles at that particular joint. This includes a reflex delay and the systems controlling flexion and extension of the muscles.

Joint stiffness and Parkinsons disease are related through a term called Parkinsonian rigidity. Rigidity is a uniform increase in muscle tone, described as a constant resistance throughout the range of passive movement and is present during all directions of movement [5]. Joint movement is only possible because all muscles have an opposing muscle. This means

that when one muscle contracts the other stretches and vice versa. With Parkinsons disease, the proper synchronization of opposing actions of the muscle pairs is impaired, resulting in all muscles remaining in the contracted state when the join is in a relaxed position [6]. This constantly-contracted state has an adverse effect on the spring-like properties of joints, altering the relationship between joint torque and joint angle and can be depicted as a constant resistance.

Since intrinsic stiffness is independent of control signals from the neural system, Parkinsonian rigidity only has an effect on reflexive stiffness. By separating and identifying the intrinsic and reflexive components of wrist stiffness, it is possible to gain a better understanding of the effect that Parkinson's disease has on the motor control system. Similar approaches have been performed on patients exhibiting spastic motions of the elbow [7] and ankle [8]. While this research is primarily performed for scientific reasons and a general understanding of the effect of Parkinsons disease on the motor control system, the method could lead to early detection of Parkinson's disease in patients not exhibiting typical symptoms, a quantitative analytical measurement of the severity of the disease, and as a testing mechanism for the effectiveness of new medicines.

The main purpose of this work was to apply the parallel pathway joint stiffness model [4] and test its validity to the wrist joint for Parkinsons disease patients. This was performed by acquiring data through the use of a test setup designed for the exdperiment, discretzing the continuous-time models in the parallel pathway model, and performing ARMAX system identification techniques to determine the models parameters. The results were then examined, thus highlighting strengths and weakness in the model.

2.0 ANALYSIS METHODS

2.1 TEST DESCRIPTION

2.1.1 Apparatus

The test setup consists of an adjustable chair, forearm splint, and servomotor used to stretch and shorten wrist muscles by applying rotational perturbations to the subject's wrist joint. The subject sits in an adjustable chair and places their hand into a U shaped channel which is connected to the servomotor, as depicted in Figure 1. The axis of the wrist joint is aligned with the shaft of the servomotor, so that rotation of the servomotors shaft produces an equivalent angular rotation of the wrist joint. The subjects arm is supported on a horizontal plane and secured in place using a vacuum bag splint to prevent forearm pronation and supination. This splint ensures that any torque measured will be purely from the flexor and extensor muscle groups that control the wrist joint. The servomotor is driven by a computer-generated pseudo-random binary sequence, as seen in 2. The displacement amplitude was 2.5 degrees in both directions. It is important that the positional rotations must be small enough to result in a linear joint stiffness characteristic, but large enough so that stiction of the wrist joint is a small contributor to the dynamic response.

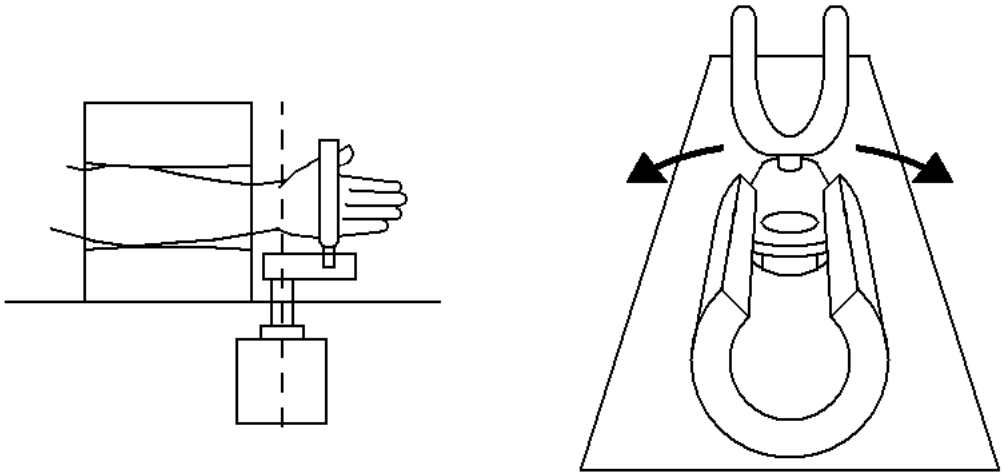

Figure 1: (a) Horizontal view of test apparatus (b) Top down view of test apparatus.

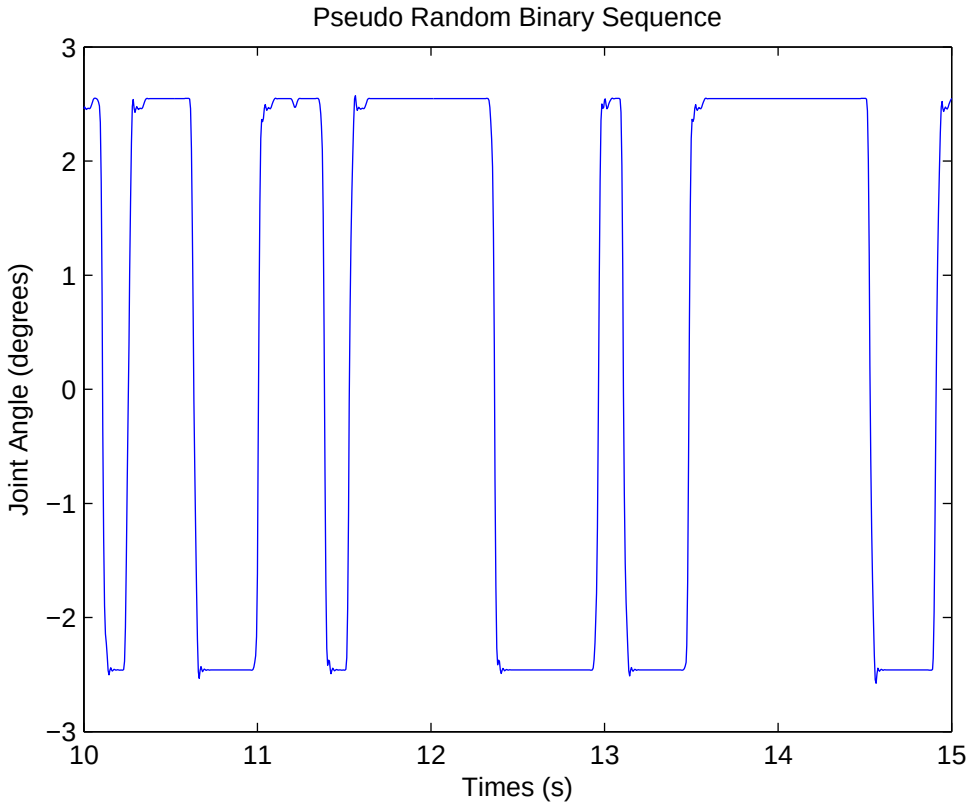

Figure 2: (Sample Psuedo Random Binary Signal (PRBS) position change.

2.1.2 Test Subjects

Ten test subjects were recruited and referred by a neurologist from the Department of Physical Therapy at Creighton University. These subjects experienced joint rigidity as a predominant symptom of Parkinsons disease. Prior to testing, the subjects were rated for severity of disability and rigidity on the unified Parkinsons disease rating scale (UPDRS) by means of a motor examination. All subjects had consented to the experiment which was approved by the Institutional Review Board of Creighton University.

2.1.3 Testing Procedure

Test subjects were asked to be seated in a chair whose height was adjusted until their forearm rested comfortably on the arm splint. Before starting the test, a neutral position, defined as zero degrees, was found by both visual alignment and passive force measurement. Next, test subjects were given practice trials to become accustomed to the device. There was a two-minute break to prevent fatigue and avoid potential habituation. Each subject was asked to completely relax the wrist muscles to their maximum capability and then the pseudo-random binary sequence was applied. To preclude a test subject from predicting a forthcoming perturbation through habituation and thus preparing a reflexive resistance before it occurs, however, prediction of a perturbation is not possible during these tests due to the pseudo-random nature in which the perturbation signal was generated.

Surface EMG signals were recorded from the flexor carpi radialis (FCR), flexor carpi ulnaris (FCU), extensor carpi radialis (ECR), and extensor carpi ulnaris (ECU) muscles using differential surface electrodes. The EMG signals were amplified by 10 and band-pass filtered with a bandwidth 20 - 450 Hz before sampling at a rate of 1 kHz per channel. The area where the electrodes were applied was properly prepared and the electrodes were placed over the belly of each muscle. Angular position and velocity were recorded using the encoder outputs from the servomotor controller. Joint torque was measured with a strain gauge torque transducer. The angular position, velocity, and joint torque were sampled at 1 kHz per channel.

2.2 PARALLEL WRIST STIFFNESS DYNAMICS

The wrist dynamics can be thought of as a parallel combination of intrinsic and reflexive contributions, as seen in Figure 3. Variations of this idea has been applied to the ankle [4], shoulder [1], and elbow [2][3]. Even though the motion for these joints and the wrist differ, it has been theorized that the same model can be used because the mechanical, muscular, and neural properties are similar.

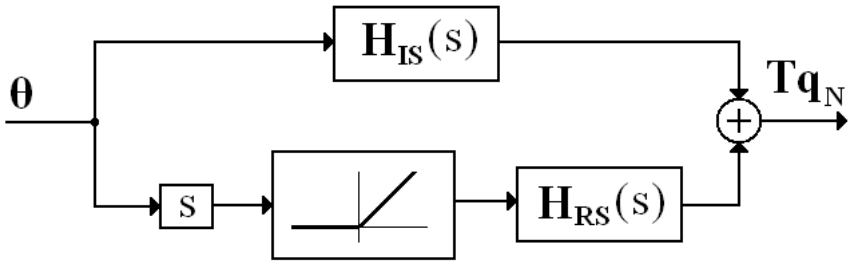

Figure 3: Parallel Pathway model for joint stiffness.

To separate intrinsic and reflexive torque and to determine the parameters for their respective systems, it is necessary to analyze position, velocity and torque signals obtained from testing. Position is the rotational position, or joint angle, of the wrist in degrees. Velocity is the speed at which the wrist gets to a position. Torque is a rotational force that causes a change in rotational motion. As it applies to this experiment, the torque is a measure of the force required to move a subjects wrist during a perturbation. The total measured torque (from the wrist) Tq is a combination of intrinsic torque, Tq_I, and the reflexive torque, Tq_R, as seen in the relationship

$$Tq = Tq_I + Tq_R. \tag{2.1}$$

2.2.1 Intrinsic Stiffness

The intrinsic component can be thought of as a measure of joint stiffness over the range of motion of the wrist joint. Parkinson's disease and other diseases that affect the central nervous system should not have an effect on any of the intrinsic stiffness parameters. However, factors such as age, past injuries and diseases that affect the tissues that act as cushions

inside the joints such as Osteoarthritis and Rheumatoid arthritis can have an affect on these parameters, therefore, patients in the study were screened for these conditions.

The intrinsic component of torque is due to the force required to overcome the intrinsic mechanisms of the wrist and is considered to be modeled by a linear, dynamic response to position with no delay [4]. Consequently, the intrinsic stiffness dynamics can be represented by the equation

$$H_{IS} = \frac{Tq_I(s)}{\theta(s)} = Is^2 + Bs + K \tag{2.2}$$

where Tq_I is intrinsic torque, θ is joint angle relative to the rest reference position, I is inertial parameter, B is viscous damping parameter, K is elastic stiffness parameter and s is Laplace variable. Since s is dependent upon frequency, K may also be considered the steady-state gain of the intrinsic stiffness system model. It is important to note that equation 2.2 presumes viscous damping, linear rotational stiffness and no stiction or other frictional losses that are not linearly related to joint velocity.

2.2.2 Reflexive Stiffness

The reflexive component of torque can be thought of as the force applied by the patient to overcome the rotational perturbation. Since Parkinson's disease affects the central nervous system which therefore affects motor control, reflexive stiffness is expected to be affected by this disease. In general, reflexive stiffness will be affected by anything that affects the supra spinal level of the motor system.

The reflexive component of torque is due to the force required to overcome the reflexive mechanisms of the wrist and is modeled as a differentiator in series with a delay, a static nonlinear element, and then a dynamic linear element [4]. The static nonlinear element is essentially a half-wave rectifier. The reasoning behind the rectifier is that flexion and extension systems are different. They both are governed by the same model but target different groups of muscles. Flexion motions target the flexor-pronator group of muscles including the carpi radialis, palmaris longus, and flexor carpi ulnaris, while extension motions target the extensor-supinator group including the extensor carpi radialis brevis, extensor

carpi radialis longus extensor carpi ulnaris. These groups of muscles differ in length and diameter and they will have different have different values for gain, damping, and natural frequency.

Reflexive stiffness linear element dynamics can be modeled as a standard second-order low-pass system in series with a delay such as

$$H_{RS} = \frac{Tq_R(s)}{V(s)} = \frac{G_R\omega_0^2}{s^2 + 2\xi\omega_0 s + \omega_0^2} e^{-st} \tag{2.3}$$

where Tq_R is reflexive torque, V is joint angular velocity, G_R is the reflexive gain, ω_0 is the natural frequency, ξ is the damping factor, t is the reflex delay, and s is the Laplace variable.

2.2.3 Reflexive Component Delay

When the wrist position is rapidly changed, there is a time delay through the bodys natural feedback system. Once a disruption has been sensed at the point of origin, the signal must travel from the point of origin to the spinal cord. Then the spinal cord will send a signal back to the muscles informing them to resist this movement. During simple movements, such as the ones used in this experiment, the spinal cord is capable of coordinating muscle activity without the help of the brain. The brain is only necessary for complex or atypical motions. In order to accurately identify the system for the reflexive component of torque, one must determine this delay from the position and electromyography data.

2.3 PARAMETER ESTIMATION

2.3.1 Discretization

The bilinear Transform maps any point on the left half of the s-plane to a point on or within the unit circle on the z-plane [9]. This complete mapping means that the bilinear transform has a good characterization of the higher frequency components of a system [10]. The bilinear transform is

$$s = \frac{du(t)}{dt} \approx \frac{2}{T}\frac{1 - z^{-1}}{1 + z^{-1}} \tag{2.4}$$

where s is the Laplace variable, T is the sampling time, and z is the shift operator for the z-domain.

However, discretization using the bilinear transform of a continuous-time system with no poles transforms the system into a discrete system with a pole in the z-domain that corresponds to an unstable pole on the $j\Omega$ axis in the s-domain [11]. For this reason, Newtons backward difference formula will be used to map derivatives used in intrinsic torque calculations to the z-domain

$$s = \frac{du(t)}{dt} \approx \frac{u(n) - u(n-1)}{T} \tag{2.5}$$

where s is the Laplace variable and T is the sampling time [12].

2.3.2 ARMAX(Autoregressive Moving Average with eXongenous inputs)

Given a set of time series data, an ARMAX model is a technique for understanding and predicting future values of the time series. This model contains an autoregressive (AR) model, a moving average model (MA), and combines linearly current and prior terms of a known, and external, time series.

The autoregressive model describes a stochastic process that can by described by a weighted sum of its previous values combined with a white noise error signal [13]. This means that a value at time t is based upon a linear combination of prior and current values. The moving average part is used as a low-pass filter in order to smooth out the time series and reduce some of the high-frequency variance, thus highlighting long-time trends [13].

It is not possible to identify time-varying parameters, therefore, the parameters must have stationary distribution within the time series being examined. Time-varying parameters can be estimated by using a recursive identification method, but in the case of wrist stiffness model, the parameters are considered stationary. It is possible that fatigue could affect the parameters over time, but the testing duration is short and test subjects are given long breaks between tests to reduce the potential for fatigue issues.

The compressed general form of an ARMAX model is: [14]

$$A(z)y(t) = B(z)u(t) + C(z)e(t) \tag{2.6}$$

This describes the I/O relationship of a linear system written as a difference equation where y is the output, u is the exogenous input and e is an uncontrolled input, such as white noise. A, B, and C are polynomials in z that represent the orders of the models. The higher the order of these polynomials, the more prior values of the time series are necessary. In the case of a time series set of data, z does not refer to the z-transform, but it is used just as a shift operator

$$z^{-1}X(k) = X(k-1) \tag{2.7}$$

After specifying the orders, least squares regression is used to find the coefficients of the polynomials which minimize the error. For the k-th entry in the time series, the error $varepsilon(k, \theta)$ is defined as

$$\varepsilon(k, \theta) = y(k) - \hat{y}(k) = y(k) - \phi(k)^T\theta \tag{2.8}$$

where $\phi(k)$ is a combination of past input and output values, θ is the vector corresponding to the parameters, y is the actual output of the system, and $\hat{y}$ is the estimated output. The above can be rewritten in vector form:

$$\begin{bmatrix} \varepsilon(1,\theta) \\ \varepsilon(2,\theta) \\ \varepsilon(3,\theta) \end{bmatrix} = \begin{bmatrix} y(1) \\ y(2) \\ y(3) \end{bmatrix} - \begin{bmatrix} \phi(1) \\ \phi(2) \\ \phi(3) \end{bmatrix} \theta \rightarrow E_N(\theta) = T_N - \Phi_N\theta. \tag{2.9}$$

Ideally, the error for the k-th term should be

$$E\left[\varepsilon(k, \theta) \mid \phi(k)\right] = 0 \tag{2.10}$$

However, the best estimate of parameters will yield the minimum of the sum of the squared prediction error

$$min_{\theta} E_N(\theta)^T E_N(\theta) \tag{2.11}$$

By means of orthogonal projection the least squared error estimator is found to be

$$\theta_{LS} = \left(\Phi_N^T \Phi_N\right)^{-1} \Phi_N^T \Phi_N Y_N \tag{2.12}$$

3.0 IDENTIFICATION METHODS

3.1 INTRINSIC STIFFNESS DYNAMICS

As described earlier, the model for the intrinsic stiffness dynamics are expressed in Eq. 2.2. However, the system identification of such a model's parameter's is difficult. The models lack of poles causes instability at high frequencies causing it to grow without bounds. Therefore, it was suggested that it was necessary to invert intrinsic stiffness dynamics and obtain its inverse, intrinsic compliance dynamics instead [4]. The resulting equation becomes

$$H_{IC}(s) = \frac{\theta(s)}{Tq_I(s)} = \frac{1}{Is^2 + Bs + K}. \tag{3.1}$$

This system resembles the well known mechanical spring where I is the mass, B is the coefficient of viscous damping parameter and K is the spring stiffness. When the intrinsic stiffness dynamics are discretized using Newtons backward formula, the intrinsic stiffness dynamics become

$$H_{IS}(z) = \left(\frac{I}{T^2} + \frac{B}{T} + K\right) + \left(-\frac{2I}{T^2} - \frac{B}{T}\right) z^{-1} \frac{I}{T^2} z^{-2} \tag{3.2}$$

which is a moving average FIR filter. Using equation 3.2, it is not necessary to find intrinsic compliance first because the system is always stable. In addition, finding intrinsic stiffness directly has an advantage over finding intrinsic compliance first. The ARMAX identification procedure, like any optimization routine, attempts to minimize the error between the actual output and the estimate. In the case of a noisy input signal, this error would be additive measurement noise. Using the intrinsic stiffness model, intrinsic torque can be described as

$$Tq_I(z) = B(z)\theta(z) + \eta_s \tag{3.3}$$

where $Tq_I(z)$ is intrinsic torque, $B(z)$ is a polynomial in z, $\theta(z)$ is joint angle, and η_S is the noise associated with intrinsic stiffness model. Using the intrinsic compliance model, joint angle can be described as

$$\theta(z) = \frac{B(z)}{A(z)} Tq_I(z) + \eta_c \tag{3.4}$$

where $Tq_I(z)$ is intrinsic torque, $B(z)$ and $A(z)$ are polynomials in z, $\theta(z)$ is joint angle, and η_C is the noise associated with intrinsic compliance model.

As stated earlier, the ARMAX identification procedure minimizes the noise during its identification of the parameters. However, the noise associated with intrinsic stiffness, η_S, is not the same as the noise associated with intrinsic compliance, η_C. If the inverse of intrinsic compliance was used as intrinsic stiffness, the models and parameters would not be optimized.

Due to the reflexive delay, it can be assumed that from the beginning of a rotational displacemtn perturbation and up until the reflexive delay of the torque response occurs, the torque is purely due to the intrinsic stiffness dynamics. Although the reflexive delay is assumed to be accurate, it is only an estimate. It is known that the first 40 ms of response to a perturbation is purely intrinsic [4] and, knowing that the intrinsic dynamics can be modeled as a FIR filter of the second order, the system response should have occurred within this 40 ms period. Consequently, an accurate identification of the intrinsic system is possible. Therefore, only the first 40 ms of torque response after a perturbation occurs is used in the identification procedure to determine the intrinsic compliance dynamics.

Since there are numerous perturbations and torque responses per test, it is necessary to create average perturbation and torque response waveforms. To create an average waveform, the segments of perturbations and torque responses were gathered separately. The waveforms were then analyzed and were chosen or rejected due to their maximum value, minimum value, and area under the curve. After outliers were removed, the waveforms were averaged together to create an average perturbation. The averaging process is beneficial because the noise in

the signal is assumed to be Gaussian white noise and the average process should minimize the noise resulting in a cleaner waveform.

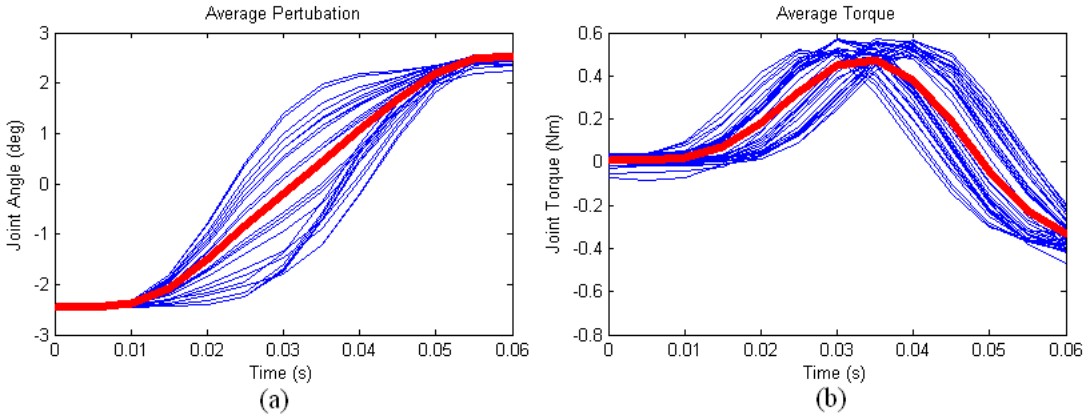

Figure 4: Average position perturbation (a) and average torque response (b).

Once the average perturbation and torque response waveforms are obtained, the ARMAX identification procedure is used to obtain an initial estimate of the intrinsic torque. Using this estimate, the ARMAX identification procedure is performed on the entire data set to find the proper order I/O relationship of the form

$$\frac{Tq_I(z)}{\theta(z)} = \left(a_0 + a_1 z^{-1} + a_2 z^{-2}\right) \tag{3.5}$$

Relating 3.2 and 3.5 and using linear algebra, it is possible find the relationship between the discrete-time and continuous time parameters:

$$\begin{bmatrix} a_0 \\ a_1 \\ a_2 \end{bmatrix} = \begin{bmatrix} \frac{1}{T^2} & \frac{1}{T} & 1 \\ -\frac{2}{T^2} & -\frac{1}{T} & 0 \\ \frac{1}{T^2} & 0 & 0 \end{bmatrix} \begin{bmatrix} I \\ B \\ K \end{bmatrix}. \tag{3.6}$$

3.2 REFLEXIVE DELAY

The delay is defined to be the time between a change in rotational position of the wrist and a corresponding spike recorded in the EMG. Since EMG signals are very noisy, due to the fact that the measurement may not come from a single muscle and that, consequently, there

is a lot of measurement noise, a spike in the EMG is only considered substantial if it passes a threshold substantially greater than the variance of the noise in the signal. This threshold is set to be two standard deviations above the mean of the EMG. Figure 5 shows an example of an EMG and the peaks located above the threshold.

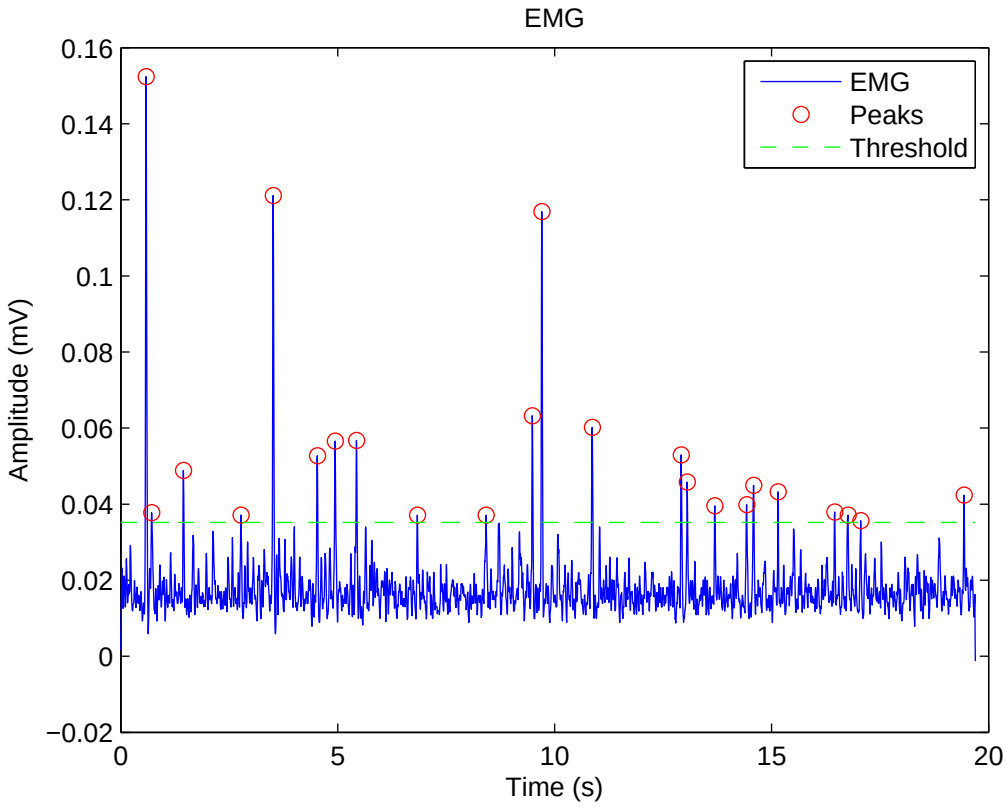

Figure 5: Typical EMG signal depicting significant peaks above a set threshold.

Each muscle may not necessarily demonstrate a spike due to each position change. Therefore, it is necessary to measure the delay associated between the position signal and all measured EMGs. The measured delays are then pooled together, outliers are removed and finally the mean of the delays is considered to be the measured delay.

This is not necessarily the true delay; it is only an estimate. The process identifies when a typical peak of a spike occurs, but that is not necessarily when the reflex occurs. It is unclear whether the actual reflex delay occurs at the peak of a spike, at the beginning or at the end. In addition, there is no way to tell the exact beginning or end of a spike. Therefore, it is necessary to test a range of delays spanning from before to after the calculated delay. The delay that yields the best fit of the data will be assumed to be the correct delay.

3.3 REFLEXIVE STIFFNESS DYNAMICS

As described previously, flexion and extension parameters are different. In order to determine the flexion and extension parameters, velocity and torque signals are half-wave rectified twice accordingly in order to separate flexion and extension torque responses. Reflexive delays may differ between the two systems, but the difference is negligible.

The second order model of the reflexive stiffness dynamics system is described by Eq. 2.3. This model is discretized using the bilinear transformation to become

$$H_{RS}(z) = \frac{Tq_R(z)}{V(z)} = \frac{b_0\left(1 + 2z^{-1} + z^{-2}\right)}{a_0 + a_1 z^{-1} + a_2 z^{-2}} z^{-}\tau \tag{3.7}$$

$$\begin{aligned} b_0 &= G_R\omega_0^2 \\ a_0 &= \tfrac{4}{T^2} + \tfrac{4\xi\omega_0}{T} + \omega_0^2 \\ a_1 &= -\tfrac{8}{T^2} + 2\omega_0^2 \\ a_2 &= \tfrac{4}{T^2} - \tfrac{4\xi\omega_0}{T} + \omega_0^2 \end{aligned} \tag{3.8}$$

The coefficients of the numerator polynomial in Eq. 3.7 must be one, two, one in order to return to the Laplace domain, with the same continuous-time system, from the z-domain. Performing the ARMAX identification procedure while using this constraint is difficult. Therefore, the data will be filtered to eliminate this constraint. The transfer function then becomes

$$H_{RS}(z) = \frac{Tq_R(z)}{V'(z)} = \frac{b_0}{a_0 + a_1 z^{-1} + a_2 z^{-2}} z^{-}\tau \tag{3.9}$$

where

$$V'(z) = \left(1 + 2z^{-1} + z^{-2}\right) V(z) \tag{3.10}$$

The continuous time delay is transformed into a discrete time delay, τ,

$$\tau = \left\lceil \frac{t}{T} \right\rceil \tag{3.11}$$

where t is the continuous time delay and T is the sampling time. Using 3.8 and 3.9 it is possible to obtain the continuous-time parameters by

$$\begin{aligned} \omega_0 &= \sqrt{\frac{a_1+\frac{8}{T^2}}{2}} \\ \xi &= \frac{(a_0-a_2)T}{8\omega_0} \\ G_R &= \frac{b_0}{\omega_0^2} \end{aligned} \tag{3.12}$$

3.4 IDENTIFICATION PROCEDURE

The parameter identification procedure is outlined below:

1. The reflexive component delay estimate is determined using the position and electromyography data according to the methods of section 3.2.
2. Parameters for the intrinsic stiffness model are then calculated, as outlined in 3.1, and an intrinsic torque estimate is calculated, $\widehat{Tq_I}$
3. Using the reflexive delay and intrinsic torque estimates, one can separate reflexive torque from the net torque,

$$\widehat{Tq_R} = Tq_N - \widehat{Tq_I} \tag{3.13}$$

   This will then be used to determine the parameters for the reflexive stiffness model, as in section 3.3, and generate a reflexive torque estimate based on that model.
4. The estimated net torque

$$\widehat{Tq_N} = \widehat{Tq_I} + \widehat{Tq_R} \tag{3.14}$$

   is now computed and the model is compared to the actual net torque by a percentage variance accounted for (%VAF) calculation. The %VAF is a measurement of the variance between an estimated signal and the actual signal,

$$\%VAF = 1 - \frac{\sum_1^N \left(Tq_N - \widehat{Tq_N}\right)^2}{\sum_1^N \left(Tq_N\right)^2} \tag{3.15}$$

where N is the length of the observation

5. A new intrinsic torque estimate is computed using

$$\widehat{Tq_I} = Tq_N - \widehat{Tq_R} \tag{3.16}$$

and the estimation procedure is repeated from step 3 using this new estimate until successive iterations did not increase %VAF.

4.0 RESULTS

4.1 DATA PREPARATION

It was suggested that there are no significant frequency components in the torque signal above 100 Hz [4][11]. For this reason, all data was first filtered at a cutoff frequency of 100 Hz using an 8^{th} order Butterworth filter to attenuate high frequency noise and was then resampled, implementing an anti-aliasing filter, at 200 Hz. All data was filtered using the same filter to ensure that the group delay, the sample delay induced by the filter, be the same for all signals. Figure 6 shows a grouping of the typical signals collected during an experiment including joint angle, joint velocity, and joint torque.

4.2 REFLEXIVE DELAY

The reflexive delay is, as it pertains to this test, the time it takes the nerves to register a position change, send the signal up to your spinal cord and return to the muscle for actions. It was measured to be the time between a position change and a significant peak in the EMG signal. Table 1 shows the results for the reflexive delay associated with each test subject. Some error is expected due to the band-pass filtering of the EMG signal outlined in 2.1.3. However, as mentioned in 3.2, delays before and after these values will be tested to eliminate this error. An example or a position change and a corresponding spike can be seen in the EMG in Figure 7, the time difference was measured as the delay.

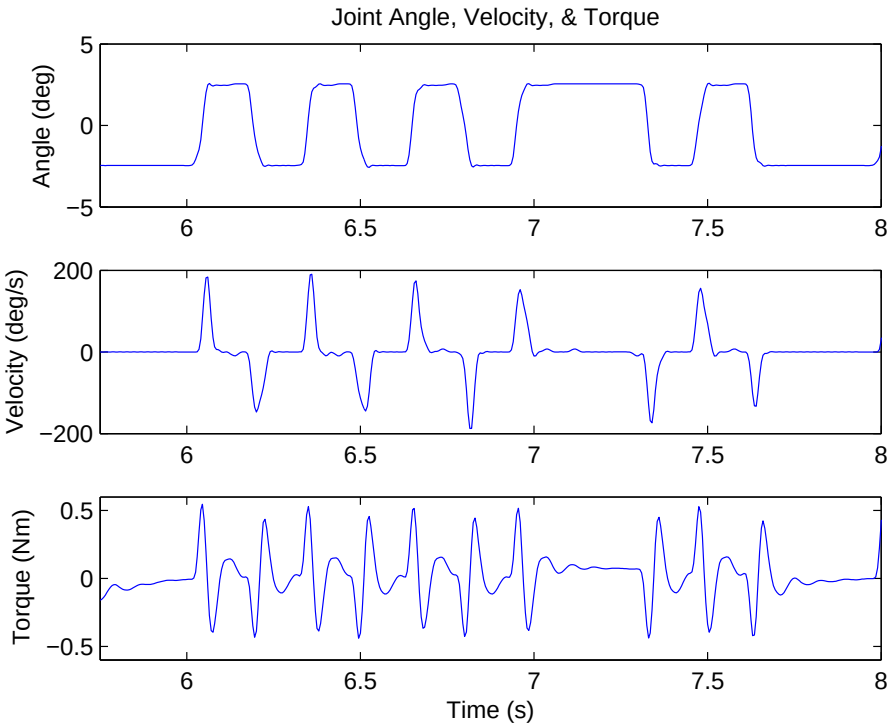

Figure 6: Typical signals collected during an experiment including joint angle, velocity, and torque.

Table 1: Table of reflexive delays

Test Subject	Delay(s)
1	0.0770
2	0.0805
3	0.0875
4	0.0745
5	0.0793
6	0.0703
7	0.0613
8	0.0569
9	0.0777
10	0.0775

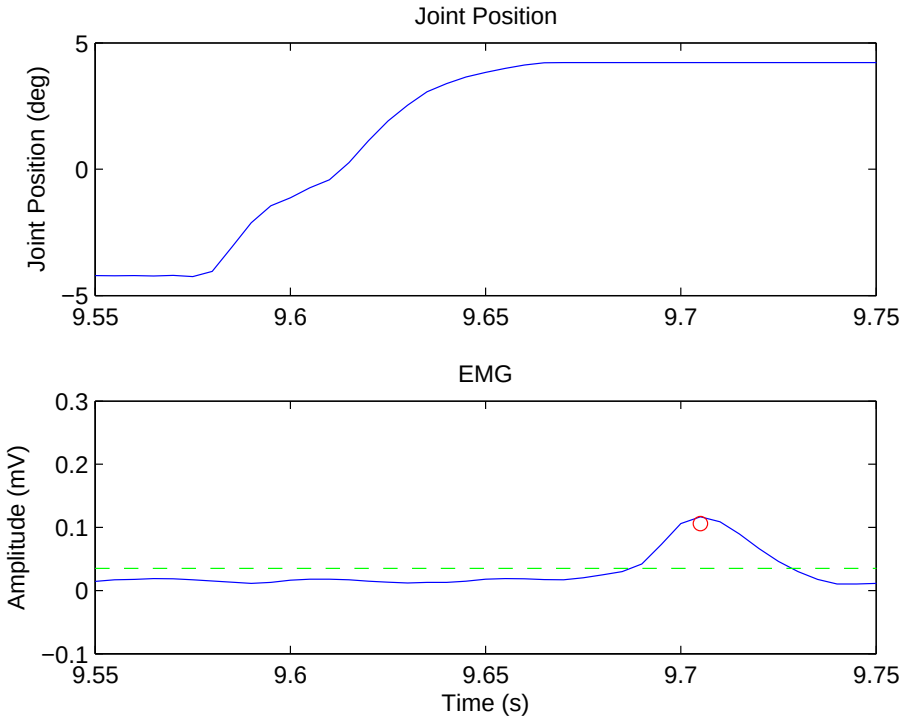

Figure 7: Beginning of a perturbation and corresponding peak in the EMG.

4.3 INTRINSIC STIFFNESS

Initially, the intrinsic stiffness parameters were to be determined by using Eq. 3.2. It became immediately apparent, as can be seen in Figure 8, that a second order FIR moving average filter was not poor fit based on the data collected, yielding a fit accuracy of less than sixty percent.

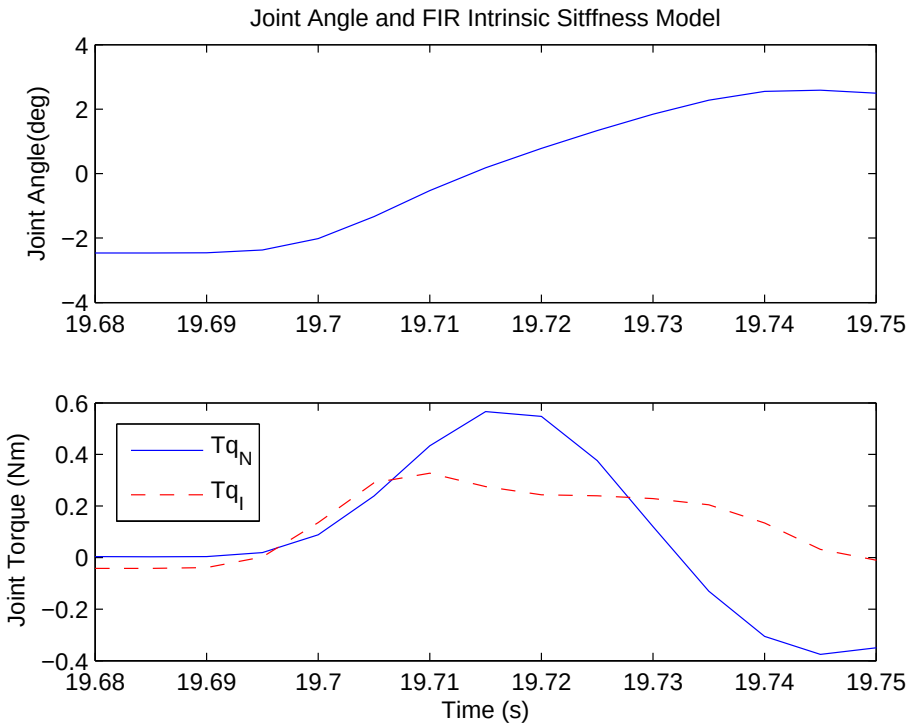

Figure 8: Joint position perturbation and corresponding torque response depicting a poor fit of the discretized intrinsic stiffness model.

It was determined that a IIR system better described the intrinsic stiffness dynamics. To determine the I, B, and K parameters, this system was then approximated by an FIR system using a new technique. Intrinsic torque can be described by the following system,

$$Tq_I(s) = \left(Is^2 + Bs + K\right)\theta(s). \tag{4.1}$$

The steady state gain K, can be found by taking the ratio of torque to position when $s = 0$,

$$K = \left.\frac{Tq_I(s)}{\theta(s)}\right|_{s=0} \tag{4.2}$$

This means, that given a substantial amount of time after perturbation, when the position has not been changed, the intrinsic response should die out leaving only the intrinsic gain steady state gain. Once K is known, then from 4.1

$$Tq_I(s) - K\theta(s) = (Is + B)\, s\theta(s) \tag{4.3}$$

Now by recognizing that $s\theta(s)$ is velocity then

$$Tq_I(s) - K\theta(s) = (Is + B)\, V(s) \tag{4.4}$$

This procedure reduces the system identification process down to the first order case. Discretization of this model is still necessary. However, it was already shown that Newtons backward formula and the bilinear transform are not good approximations to a derivative, so for this case, a higher order approximation is necessary. By definition,

$$s = j\Omega \tag{4.5}$$

where Ω is the continuous-time frequency and the corresponding continuous-time filter is

$$H(e^{j\Omega}) = j\Omega, for|\Omega| \geq \pi \tag{4.6}$$

The discrete approximation of Eq. 4.6 will be of the form

$$H_N(z) = \sum_{n=1}^{N} \frac{a_n}{2} \left(z^n - z^{-n}\right) \tag{4.7}$$

where N is the order of the approximation. By substituting $z = e^{j\Omega}$ and then using Eulers identity, the following expression is obtained

$$H_N(e^{j\Omega}) = j \sum_{n=1}^{N} a_n \sin n\Omega \tag{4.8}$$

By comparing the continuous time filter with the discrete approximation, it can be seen that

$$\Omega \approx \sum_{n=1}^{N} a_n \sin n\Omega \tag{4.9}$$

Expansion of the right-hand side of equation 4.9 using a Taylor series results in

$$\Omega \approx \sum_{n=1}^{N} a_n n^{(2m+1)} \sum_{m\geq 0} (-1)^m \frac{\Omega^{2m+1}}{2m+1} \tag{4.10}$$

$$\Omega \approx \sum_{n=1}^{N} a_n \left[n\Omega - \frac{n^3\Omega^3}{3!} + \frac{n^5\Omega^5}{5!} - \ldots\right] \tag{4.11}$$

$$\Omega \approx \sum_{n=1}^{N} a_n C_1 \Omega - C_3 \Omega^3 + C_5 \Omega^5 - \dots \tag{4.12}$$

$$C_n = \begin{cases} 1 & \text{if } n = 1 \\ 0 & \text{if } n \neq 1 \end{cases} \tag{4.13}$$

Through linear combinations of the elements it is possible to determine the $a_n s$

$$\begin{bmatrix} 1 \\ 0 \\ 0 \\ \vdots \end{bmatrix} = \begin{bmatrix} 1 & 2 & 3 & \dots \\ 1 & 2^3 & 3^3 & \dots \\ 1 & 2^5 & 3^5 & \dots \\ \vdots & \vdots & \vdots & \ddots \end{bmatrix} \begin{bmatrix} a_1 \\ a_2 \\ a_3 \\ \vdots \end{bmatrix} \tag{4.14}$$

With this method, it is possible to generate any order approximation. Figure 9 shows the differentiating filters magnitude frequency response up to a 5^{th} order approximation. As can be seen, increasing the order improves the approximation to a true derivative, but comes at a cost of increasing filter coefficients and, consequently, more values from the time series.

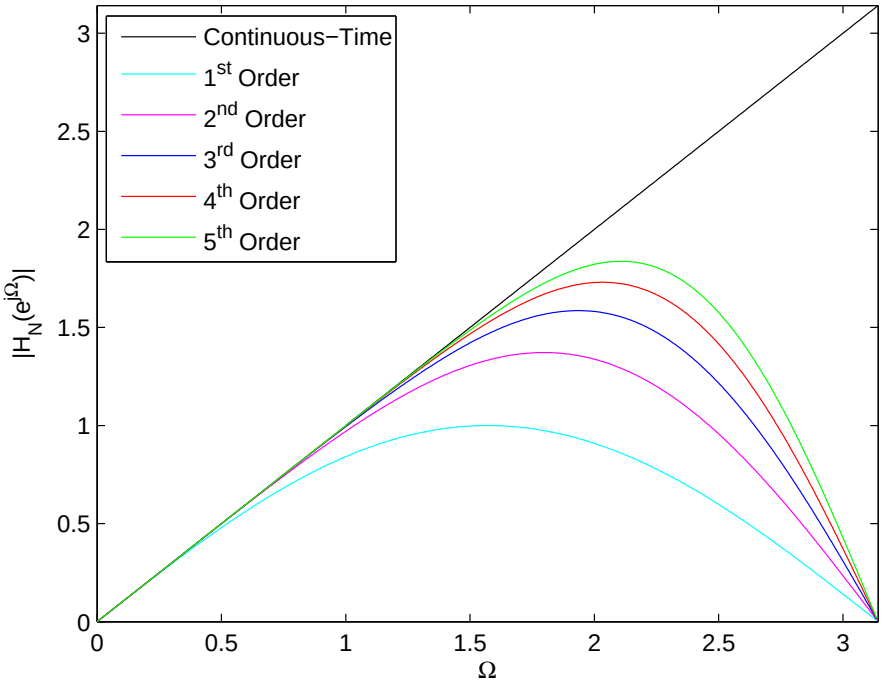

Figure 9: Comparison of actual derivative to discrete approximations.

Returning back to equation 4.4, the discrete domain derivative approximation replaces the s variable. As an example, the 2^{nd} order approximation this becomes

$$\frac{Tq(z) - K\theta(z)}{V(z)} = I\left(\sum_{n=1}^{2} \frac{a_n}{2T}\left(z^n - z^{-n}\right)\right) z^{-2} + B \tag{4.15}$$

The ARMAX procedure only works with causal systems so the coefficients of the derivative approximation must be shifted in order to make the approximation causal.

$$\frac{Tq(z) - K\theta(z)}{V(z)} = I\left(\frac{a_1}{2T}z - \frac{a_1}{2T}z^{-1} + \frac{a_2}{2T}z^2 - \frac{a_2}{2T}z^{-2}\right) z^{-2} + B \tag{4.16}$$

$$\frac{Tq(z) - K\theta(z)}{V(z)} = I\left(\frac{a_1}{2T}z^{-1} - \frac{a_1}{2T}z^{-3} + \frac{a_2}{2T} - \frac{a_2}{2T}z^{-4}\right) + B \tag{4.17}$$

$$\frac{Tq(z) - K\theta(z)}{V(z)} = \left(\frac{a_2}{2T}I + B\right) + \left(\frac{a_1}{2T}z^{-1} - \frac{a_1}{2T}z^{-3} - \frac{a_2}{2T}z^{-4}\right) \tag{4.18}$$

Parameter identification using the ARMAX procedure yields an I/O relationship of the form

$$\frac{Tq(z) - K\theta(z)}{V(z)} = c_0 + c_1 z^{-1} + c_3 z^{-3} + c_4 z^{-4} \tag{4.19}$$

where c_2 has been set to zero to correspond with the discrete approximation of the derivative. Relating equation 4.18 to equation 4.19, it is possible to determine the parameters I and B as

$$I = \frac{c_1 + c_3 + c_4}{b_1 + b_3 + b_4} \tag{4.20}$$

$$B = c_0 - Ib_0 \tag{4.21}$$

The equation for B, 4.21, will remain the same for any N order approximation of s, but the parameter I can be generalized to

$$I = \frac{\sum_{n \neq N} c_n}{\sum_{n \neq N} b_n} \tag{4.22}$$

To gather accurate representations of intrinsic torque and the steady-state gain K, the identification procedure was first performed using a IIR system that yielded good results in place of the intrinsic stiffness dynamics

$$\frac{Tq_I(z)}{\theta(z)} = \frac{b_0 + b_1 z^{-1} + b_2 z^{-2}}{a_0 + a_1 z^{-1} + a_2 z^{-2}} \tag{4.23}$$

Once successive iterations of the identification procedure failed to make significant improvements, the resulting intrinsic torque and steady state gain K found were used to identify the parameters I and B. Figure 10 shows a typical intrinsic torque signal obtained from the identification procedure.Table 2 shows the I, B, and K parameters for each of the ten test subjects. A $3^{textrmrd}$ order discrete approximation to the derivative was used to determine the coefficients as outlined above.

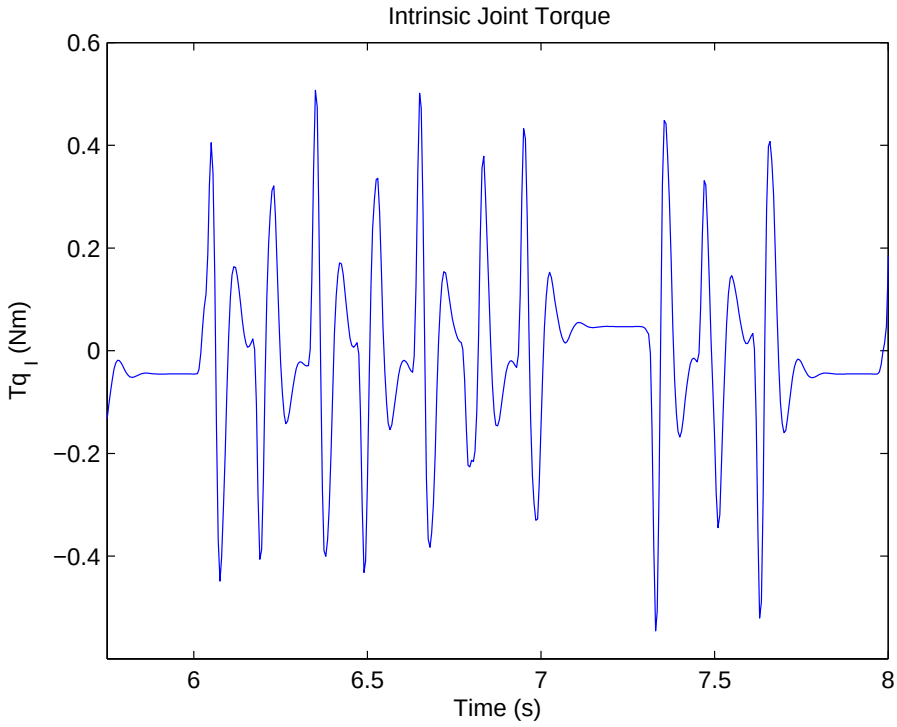

Figure 10: Typical intrinsic torque signal derived from identification procedure.

Table 2: Table of intrinsic stiffness parameters.

Test Subject	$I(Nm/s^2/deg)$	$B(Nm/deg/s)$	$K(Nm/deg)$
1	277.0941	0.00035323	0.031098
2	175.0191	00033576	0.023278
3	91.7434	-0.00013886	0.0078602
4	248.9691	0.00018931	0.022131
5	220.162	-6.7238e-006	0.0068905
6	210.2832	0.00022184	0.013271
7	-3461.8371	0.088658	0.015227
8	144.7799	0.00030566	0.017641
9	200.562	0.00037608	0.02328
10	169.7191	1.8142e-005	0.014461

4.4 REFLEXIVE STIFFNESS

In tandem with identifying the intrinsic stiffness parameters, the reflexive stiffness parameters are determined. The reflexive stiffness dynamics are only attributed to the neural systems response to a perturbation. Reflexive stiffness parameters for flexion can be seen in Table 3 and for extension in Table 4.

Table 3: Reflexive Stiffness Parameters for flexion motions.

Test Subject	G_R	ξ	ω_0
1	-3.3486e-013	3.354e-008	399.9988
2	1.1351e-012	7.043e-008	399.9988
3	-2.0765e-012	6.2722e-008	399.9988
4	-1.4184e-014	3.024e-009	399.9988
5	-2.5381e-012	4.5278e-008	399.9988
6	-6.7441e-013	4.5331e-008	399.9988
7	5.1146e-009	3.5749e-010	399.999
8	6.8288e-013	2.7966e-006	400.0001
9	-1.5108e-012	4.5676e-008	399.9989
10	-4.1262e-012	3.0446e-008	399.9989

The results for the reflexive torque parameters are very peculiar. In every instance, the natural frequency is near identical while the reflexive gain and damping factor change. While this could be a characteristic of Parkinsons disease it is extremely unlikely. In addition, the reflexive gain in is extremely smals, implying that intrinsic wrist stiffness is dominant. The

Table 4: Reflexive Stiffness Parameters for extension motions.

Test Subject	G_R	ξ	ω_0
1	9.9364e-013	4.6632e-008	399.9988
2	-3.2519e-012	3.1629e-008	399.9989
3	7.7576e-013	4.2002e-008	399.9988
4	-2.0859e-012	1.8573e-008	399.9989
5	-3.6761e-012	4.5581e-008	399.9988
6	1.8086e-012	1.1889e-007	399.9988
7	1.3833e-008	2.8085e-009	399.999
8	-1.0725e-011	5.0065e-008	399.999
9	6.4797e-013	2.9852e-009	399.9989
10	-8.2285e-012	6.0816e-008	399.999

results do show that reflexive gain, G_R, and the damping factor, ξ, are different for flexion and extension confirming the prior belief that flexion and extension systems are different.

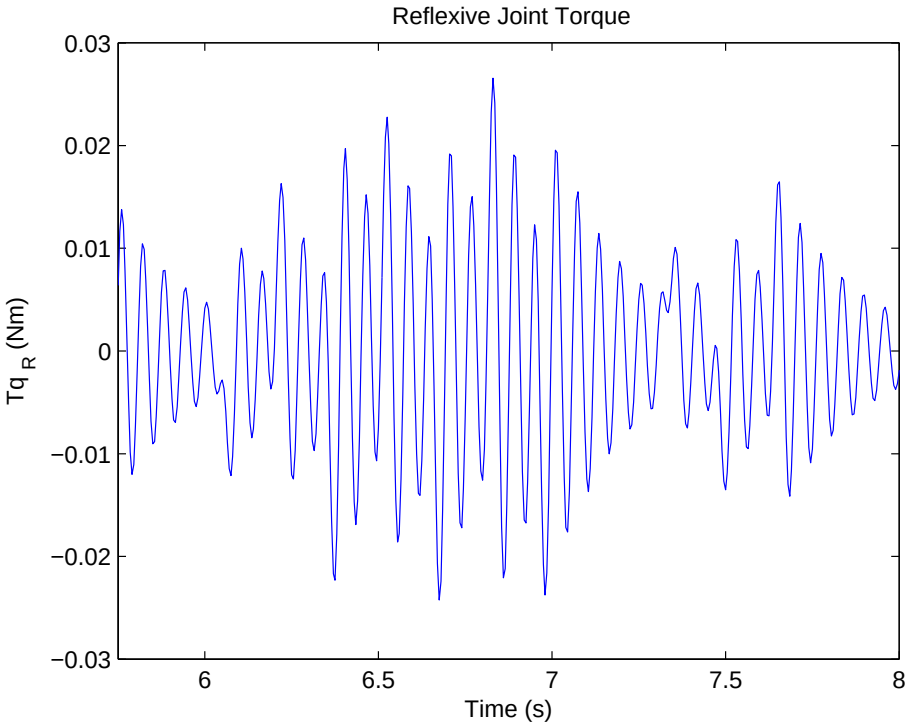

Figure 11: Typical reflexive torque signal derived from identification procedure.

An example reflexive torque signal is shown in Figure 11. The figure shows an oscillating wave at a much high frequency than that of intrinsic torque. This oscillation can be attributed to the most prominent sign of Parkinsons disease, the hand tremor. Since the tremor is not produced by anything intrinsically, its cause is purely reflexive. A normal hand tremor is in the range of 3 to 8 Hz when the hand is at rest [15]. In contrast, the range of tremor from these results are in the range of 15 to 20 Hz. It is likely that the higher frequency range from these results is due to the fact that the hand is not at rest, but moving according to the position change. It is also apparent from Figure 12 that the tremor is of greatest magnitude directly following a perturbation, after which it begins to decay. This can be associated with action tremor which increases with movement and lessens with rest [15].

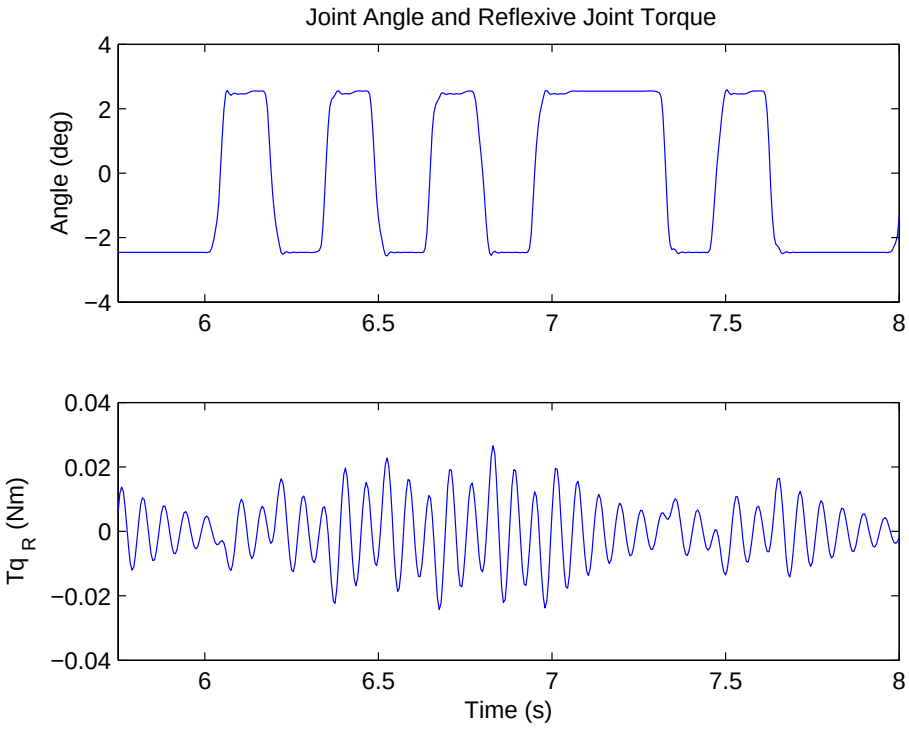

Figure 12: Perturbations and the corresponding reflexive torque signal.

4.5 NET TORQUE

The total effectiveness of the parallel pathway model and the identification procedure can be seen in Table 5. Overall, the procedure did a good job in estimating torque , only in two instances did the identification procedure perform worse than 75% VAF. However, in one of the two instances, the results failed to converge and did not provide any useful measure of estimated torque.

Table 5: $\%VAF$ values for the experiments.

Test Subject	%VAF
1	77.73
2	88.47
3	43.04
4	85.23
5	75.89
6	83.33
909 7	< 0
8	86.45
9	86.81
10	85.78

Figure 13 compares actual net torque, Tq_N, and the net torque estimate, $\widehat{Tq_N}$, from the identification procedure. While the estimated torque is reasonably close to the actual torque, in more than a few instances the peaks do not match. This may imply that there are some higher frequency components that were not accounted for in the estimation.

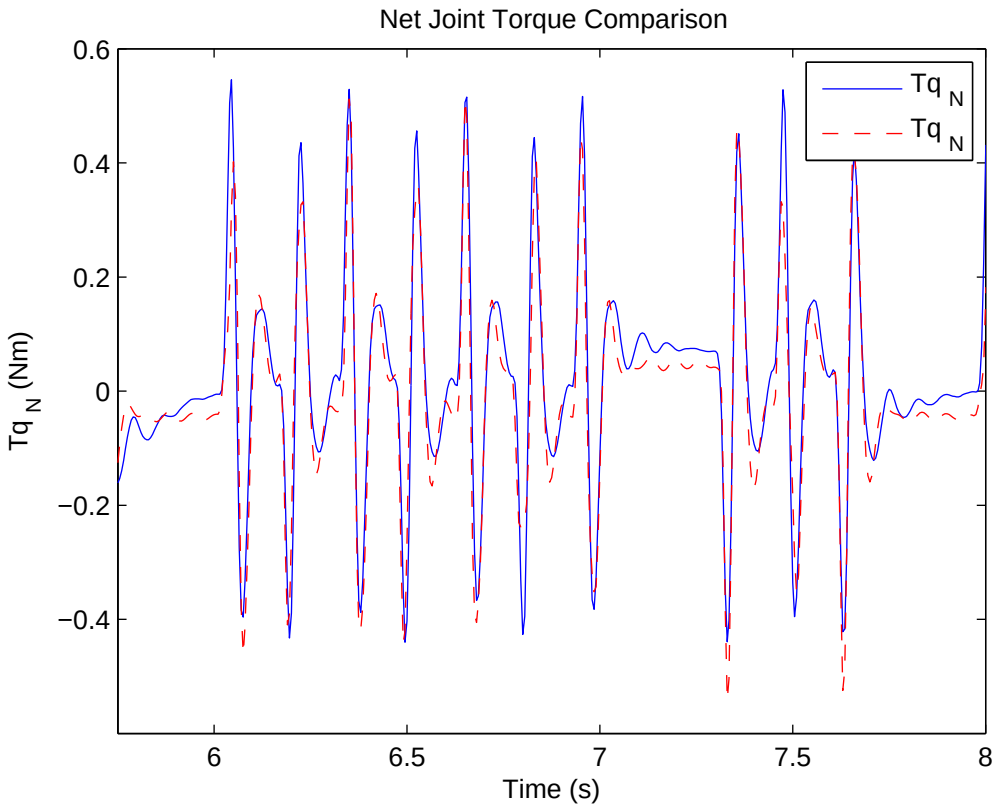

Figure 13: Comparison of actual net torque and estimated net torque.

5.0 DISCUSSION AND CONCLUSION

The parallel pathway for joint stiffness model has been proven to work well for joints such as the ankle and the results for the experiments conducted for this research indicate that the same is true for wrist stiffness in Parkinson's disease patients. It is my belief that with some improvements, the parallel pathway joint stiffness model would be appropriate for characterising the intrinsic and reflexive stiffness dynamics of a Parkinsons disease patients wrist joint.

Adding poles to the system for intrinsic stiffness, changing the system into an IIR system, drastically improved the results. This implies that the intrinsic stiffness dynamics may be better described by an IIR system [2] [1]. Furthermore, increasing the order of the IIR system used to find intrinsic torque did not improve the results. This also suggests that the system used to determine intrinsic torque is a better system than the one used in the parallel pathway model.

It has also been shown that the model for the reflexive stiffness dynamics may be incorrect [1][16][17], but based upon the high %VAF of net torque produced from the evaluated reflexive stiffness system it is likely that the model tested is appropriate. However, this is difficult to discern because the identification procedure hinges on a correct estimation of the intrinsic stiffness dynamics. If the intrinsic stiffness dynamics estimate from the first 40 ms of a perturbation response is governed by the wrong model, some intrinsic stiffness dynamics will be attributed to the reflexive stiffness dynamics.

The reflexive stiffness dynamics depicted parkinsonian hand tremor as seen in Figure 11. Although the frequency was higher than what is expected of resting tremor, it was determined that this could be attributed to the rapid change in position resulting in what is known as an action tremor. As expected, the action tremor was greatest during movement and decreased with rest as seen in Figure 12.

Something that may reduce the effectiveness of this procedure is that the systems described in the parallel pathway model are all continuous-time. The discretization methods used are not perfect and there is some error associated with each of them. For instance, Newtons backward formula does not map the left hand side of the s plane on to the entire unit circle. While the bilinear transformation is able to map the entire jΩ-axis in the s-plane to one revolution of the unit circle in the z-plane, the transformation between the continuous-time and discrete-time frequency is nonlinear with respect to frequency [9]. This problem is usually counteracted by pre-warping the frequency axis but, the desired continuous-time or discrete-time frequencies variables must be known for an effective warping. In the case of system identification, these variables are not known thus, pre-warping can not be performed.

A strong concern is how Parkinsons disease affects the validity of the identification method. As described earlier, Parkinsons disease affects the central nervous system, which in turn, has an effect on motor control. Parkinsonian rigidity, one characteristic of Parkinsons disease, places the muscles acting on a joint in constant contraction. This means that the muscles contribute to the resistance when a perturbation occurs, despite their pseudo random nature. Knowing this, it can be assumed that the initial guess of the intrinsic stiffness dynamics based upon the first 40 ms after a perturbation contains some reflexive components. If this is true, it is impossible to separate intrinsic and reflexive torque as described in this method. This conclusion is supported by my results. The reflexive gain is so small that the reflexive stiffness is negligible when considering the entire system. This implies that all wrist joint stiffness is attributable to intrinsic properties only or that reflexive components are included with the intrinsic stiffness results, the latter is more likely. It is clear that another way of separating intrinsic and reflexive stiffness components is necessary.

One possible way to separate intrinsic and reflexive contributions to the wrist stiffness dynamics is to first have a patient use medication to reduce the symptoms of Parkinsons disease and then perform the experiment. The intrinsic stiffness dynamics determined from the experiment could then be combined with data from an experiment where the patient was not administered medication. Then analysis of the combined data could lead to accurate representations of intrinsic and reflexive stiffness. Another idea is to perform system identification on the entire model at once. From the techniques described in this paper, it is not possible due to the ARMAX procedures dependence on linear terms and nonlinearity of the reflexive pathway. However, NARMAX [11] and other nonlinear system identification techniques, Wiener kernel approaches [18] and Hammerstein cascade models [19] could be used and will be investigated.

Despite some flaws in the procedure and model, it was still possible to obtain reasonable results using the parallel pathway model. With some alterations, the parallel pathway model could be used to identify intrinsic and reflexive components to wrist stiffness in Parkinsons disease patients. From this, it would be possible to gain a better understanding of the problems associated with Parkinson's disease and develop new diagnosis techniques and medicines.

BIBLIOGRAPHY

[1] F. C. T. van der Helm, A. C. Schouten, E. de Vlugt, and G. G. Brouwn, "Identification of intrinsic and reflexive components of human arm dynamics during postural control," *J Neuroscience Methods*, vol. 119, pp. 1–14, 2002.

[2] F. Popescu, J. M. Hidler, and W. Z. Rymer, "Elbow impedance during goal-directed movements," *Exp Brain Res*, vol. 152, pp. 17–28, 2003.

[3] D. A. Kistemaker, A. J. V. Soest, and M. F. Bobbert, "Equilibrium point control cannot be refuted by experimental reconstruction of equilibrium point trajectories," *J Neurophysiol*, vol. 98, pp. 1075–1082, 2007.

[4] R. E. Kearney, R. B. Stein, and L. Parameswaian, "Identification of intrinsic and reflex contributions to human ankle stiffness dynamics," *IEEE Trans. Biomed. Eng.*, vol. 44, pp. 493–504, June 1997.

[5] *Parkinsons Disease & Movement Disorders*. Lippincott Williams & Wilkins, 2002.

[6] *Handbook of Parkinsons Disease*, 3rd ed. New York, NY: Marcel Dekker, 2003.

[7] M. M. Mirbagheri, C. Tsao, and W. Z. Rymer, "Abnormal intrinsic and relexive stiffness related to impaired voluntary movement," *Proc. IEEE EMBS*, vol. 26, pp. 4680–4683, September 2004.

[8] M. M. Mirbagheri, H. Barbeau, M. Ladouceur, and R. Kearney, "Intrinsic and reflex stiffness in normal and spastic, spinal cord injured subjects," *Exp Brain Res*, vol. 141, pp. 446–459, 2001.

[9] *Discrete-Time Signal Processing*, 2nd ed. Upper Saddle River, NJ: Prentice Hall, 1999.

[10] S. S. Haykin, "A unified treatment of recursive digital filtering," *IEEE Trans. Automat. Contr.*, vol. AC-17, p. 113116, 1972.

[11] S. L. Kukreja, H. L. Galiana, and R. E. Kearney, "Narmax representation and identification of ankle dynamics," *IEEE Trans. Biomed. Eng.*, vol. 50, pp. 70–81, January 2003.

[12] *CRC Standard Mathematical Tables and Formulae.* Chapman & Hall/CRC Press LLC, 2003.

[13] *Probability and Random Processes with Applications to Signal Processing*, 3rd ed. Upper Saddle River, NJ: Prentice Hall, 2002.

[14] *System Identification: Theory for the User*, 2nd ed. Upper Saddle River, NJ: Prentice Hall, 1999.

[15] *Parkinsons Disease.* Baltimore, MD: The Johns Hopkins University Press, 1990.

[16] M. M. Mirbagheri and R. E. Kearney, "Mechanisms underlying a third-order parametric model of dynamic reflex stiffness," *Proc. IEEE EMBS*, vol. 22, pp. 1241–1242, July 2000.

[17] M. M. Mirbagheri, R. E. Kearney, H. Barbeau, and M. Ladouceur, "Parametric modeling of the reflex contribution to dynamic ankle stiffness in normal and spinal cord injured subjects," *Proc. IEEE EMBS*, vol. 17, pp. 1241–1242, September 1995.

[18] M. J. Korenberg and I. W. Hunter, "The identification of nonlinear biological systems: Wiener kernel approaches," *Ann. Biomed. Eng.*, vol. 18, pp. 629–654, 1990.

[19] I. W. Hunter and M. J. Korenberg, "The identification of nonlinear biological systems: Wiener and hammerstein cascade models," *Biol. Cybern.*, vol. 55, pp. 135–144, 1986.